The Rad5 Helicase and RING Domains Contribute to Genome Stability through their Independent Catalytic Activities

Robert Toth [1,2], David Balogh [3], Lajos Pinter [4], Gabor Jaksa [4], Bence Szeplaki [4], Alexandra Graf [3], Zsuzsanna Gyorfy [1], Marton Zs. Enyedi [3,4], Erno Kiss [3], Lajos Haracska [3,†] and Ildiko Unk [1,*,†]

*1 - **DNA Repair Research Group,** Institute of Genetics, Biological Research Centre, Szeged, Eotvos Loránd Research Network, Szeged H-6726, Hungary*
*2 - **University of Szeged,** Doctoral School of Biology, Hungary*
*3 - **HCEMM-BRC Mutagenesis and Carcinogenesis Research Group,** Institute of Genetics, Biological Research Centre, Szeged, Eotvos Loránd Research Network, Szeged H-6726, Hungary*
*4 - **Delta Bio 2000 Ltd.,** Szeged H-6726, Hungary*

Correspondence to Ildiko Unk: Biological Research Centre, Temesvari krt. 62., Szeged H-6726, Hungary. *unk.ildiko@brc.hu (I. Unk)*
https://doi.org/10.1016/j.jmb.2021.167437
Edited by Titia Sixma

Abstract

Genomic stability is compromised by DNA damage that obstructs replication. Rad5 plays a prominent role in DNA damage bypass processes that evolved to ensure the continuation of stalled replication. Like its human orthologs, the HLTF and SHPRH tumor suppressors, yeast Rad5 has a RING domain that supports ubiquitin ligase activity promoting PCNA polyubiquitylation and a helicase domain that in the case of HLTF and Rad5 was shown to exhibit an ATPase-linked replication fork reversal activity. The RING domain is embedded in the helicase domain, confusing their separate investigation and the understanding of the exact role of Rad5 in DNA damage bypass. Particularly, it is still debated whether the helicase domain plays a catalytic or a non-enzymatic role during error-free damage bypass and whether it facilitates a function separately from the RING domain. In this study, through *in vivo* and *in vitro* characterization of domain-specific mutants, we delineate the contributions of the two domains to Rad5 function. Yeast genetic experiments and whole-genome sequencing complemented with biochemical assays demonstrate that the ubiquitin ligase and the ATPase-linked activities of Rad5 exhibit independent catalytic activities in facilitating separate pathways during error-free lesion bypass. Our results also provide important insights into the mutagenic role of Rad5 and indicate its tripartite contribution to DNA damage tolerance.

Introduction

DNA damage tolerance (DDT) pathways ensure the continuation of DNA synthesis despite replication-stalling DNA damage that can lead to fork collapse and cell death without further action. DDT can be error-free or error-prone depending on the actual mechanism, contributing to genomic stability or increasing the mutational burden of the genome, respectively. The Rad6/Rad18 ubiquitin conjugase/ligase complex controls error-free and error-prone DDT in the budding yeast *Saccharomyces cerevisiae* (*Sc.*). It monoubiquitylates proliferating cell nuclear antigen (PCNA) the processivity factor of replicative DNA polymerases on its lysine 164 (K164).[1,2]

Monoubiquitylated PCNA promotes the replacement of the replicative DNA polymerase by translesion synthesis (TLS) polymerases capable of inserting nucleotides opposite DNA damage.[3,4] Two different TLS subpathways have been identified for the bypass of ultraviolet (UV) light lesions. One of them is error-free executed by the *RAD30*-encoded Polη that seems to be uniquely specialized in the efficient and error-free bypass of pyrimidine dimers, the most frequent UV-induced DNA lesions.[5,6] The other is an error-prone pathway involving the Rev3/Rev7 formed Polζ, the Rev1, and the Def1 proteins. In the Polζ complex, Rev3 has the catalytic activity, whereas Rev7 is an accessory subunit.[7] Polζ is highly efficient in extending mismatched primer termini resulting from the insertion of incorrect nucleotides opposite DNA damage by other polymerases, contributing to error-prone DNA synthesis.[8,9] The enzymatic activity of Rev1 is limited, being capable of incorporating only cytosines (C) during DNA synthesis leading to error-prone bypass in most cases; however, its dominant role in TLS is considered to be structural.[8,10,11] Def1 does not have polymerase activity, but it promotes the polymerase exchange step at stalled replication forks.[12]

Polyubiquitylation of PCNA on K164 already monoubiquitylated by Rad6/Rad18 activates a third subpathway that employs template switching for the error-free bypass of DNA damage.[2,13] This branch depends on the Rad5 ubiquitin ligase and the Mms2/Ubc13 ubiquitin conjugase, which form a complex assembled through direct interaction between Rad5 and Ubc13.[1,14–16] This multiprotein complex can build a polyubiquitin chain on monoubiquitylated PCNA through lysine 63 of ubiquitin.[17] Despite its indispensable role in the *MMS2*-dependent pathway, the function of PCNA polyubiquitylation in DNA damage bypass is still elusive. Furthermore, *rad5* mutants are considerably more sensitive to DNA damaging agents than *mms2* or *ubc13* strains suggesting that Rad5 has other functions independent of Ubc13/Mms2. Indeed, in addition to the RING-finger domain essential for the ubiquitin ligase activity, Rad5 possesses a helicase domain characteristic of the DNA-dependent ATPases of the SWI2/SNF2 protein superfamily.[18] The helicase domain confers double-stranded DNA-stimulated ATPase, DNA translocase, and DNA remodeling activities, enabling Rad5 to reverse replication fork-like structures and promote strand invasion, the two possible mechanisms of template-switching.[19,20] Considering its enzymatic activities conferred by the RING and helicase domains, Rad5 was suggested to play a role in both the polyubiquitylation and the template-switching steps of the error-free bypass. This model was supported by independent studies suggesting that the two domains played separate roles in the replication of adozelesin-treated DNA and the repair of DNA double-strand breaks.[21,22] Nevertheless, the substantive function of the helicase domain and its enzymatic contribution to error-free DNA damage bypass has been questioned. It was reported that both the RING and helicase domains of Rad5 worked exclusively in connection with *UBC13* in response to methyl methanesulfonate (MMS) treatment.[23] Another study concluded that the sole function of the helicase domain in the Rad6/Rad18 governed DDT was non-catalytic, where it facilitated the Rad5-Ubc13 interaction for PCNA polyubiquitylation.[24] An essential non-enzymatic contribution of the helicase domain to error-free DDT, via supporting the interaction of Rad5 with PCNA and Ubc13 for PCNA polyubiquitylation, was reported by others, also.[25]

Rad5, like its human orthologs, the helicase-like transcription factor (HLTF) and SNF2 Histone Linker PHD RING Helicase (SHPRH) tumor suppressors, plays a pivotal role in guarding genomic stability. Besides the sequence homology, these proteins share high similarity in their domain structure, with all three having a RING domain situated in the middle of a conserved helicase domain.[26] Like Rad5, HLTF and SHPRH also function as ubiquitin ligases in PCNA polyubiquitylation and exhibit ATPase activity that promotes DNA and protein remodeling in the case of HLTF.[27–32] These data suggested that the three proteins exert similar roles in the replication of damaged DNA using these activities. Therefore, it is of great importance to unravel the molecular steps of their actions. However, the conflicting results of the literature regarding the enzymatic contribution of the Rad5 helicase domain to DNA damage bypass preclude the synthesis of a consistent model. One reason for the contradictions lies in the particular arrangement of the RING and helicase domains, making the selection of domain-specific mutations inactivating only the corresponding enzymatic activity elaborate. Therefore, applying direct assays that check the mutant proteins for both the ubiquitin ligase and the DNA remodeling activities, is rudimentary. In this study, our goal was to perform a comprehensive investigation of Rad5 to better understand its contribution to DDT. Through dissecting the roles of the RING and the helicase domains we also aimed to address the contradictions of the literature.

Results and Discussion

Selecting mutations inactivating the helicase or the RING domain of Rad5

To investigate the contribution of the helicase and the RING domains of Rad5 to its role in DNA damage bypass, we planned to characterize domain-specific mutants. To address the contradictions of the literature, we included those mutations that were used in reports concluding an essential role for the helicase domain in PCNA

polyubiquitylation through its non-enzymatic contribution to the Rad5-Ubc13 interaction. We engineered two mutations in each domain affecting distinct conserved amino acids regarded indispensable for the functionality of the given domain (Figure 1(A)). Lysine-538 in the conserved GKT motif of the Walker A box involved in ATP-binding was changed to alanine in the ATPase mutant *rad5-KA*.[33] The *rad5-DEAA* mutant had alanine substitutions in the DExx motif of the Walker B box in the ATP-hydrolyzing domain at asparagine-681 and glutamine-682 residues, inactivating both the ATP-hydrolyzing and the DNA remodeling activities of Rad5, as we have previously demonstrated.[20,34] To impair the ubiquitin ligase activity of Rad5, we mutated residues necessary for

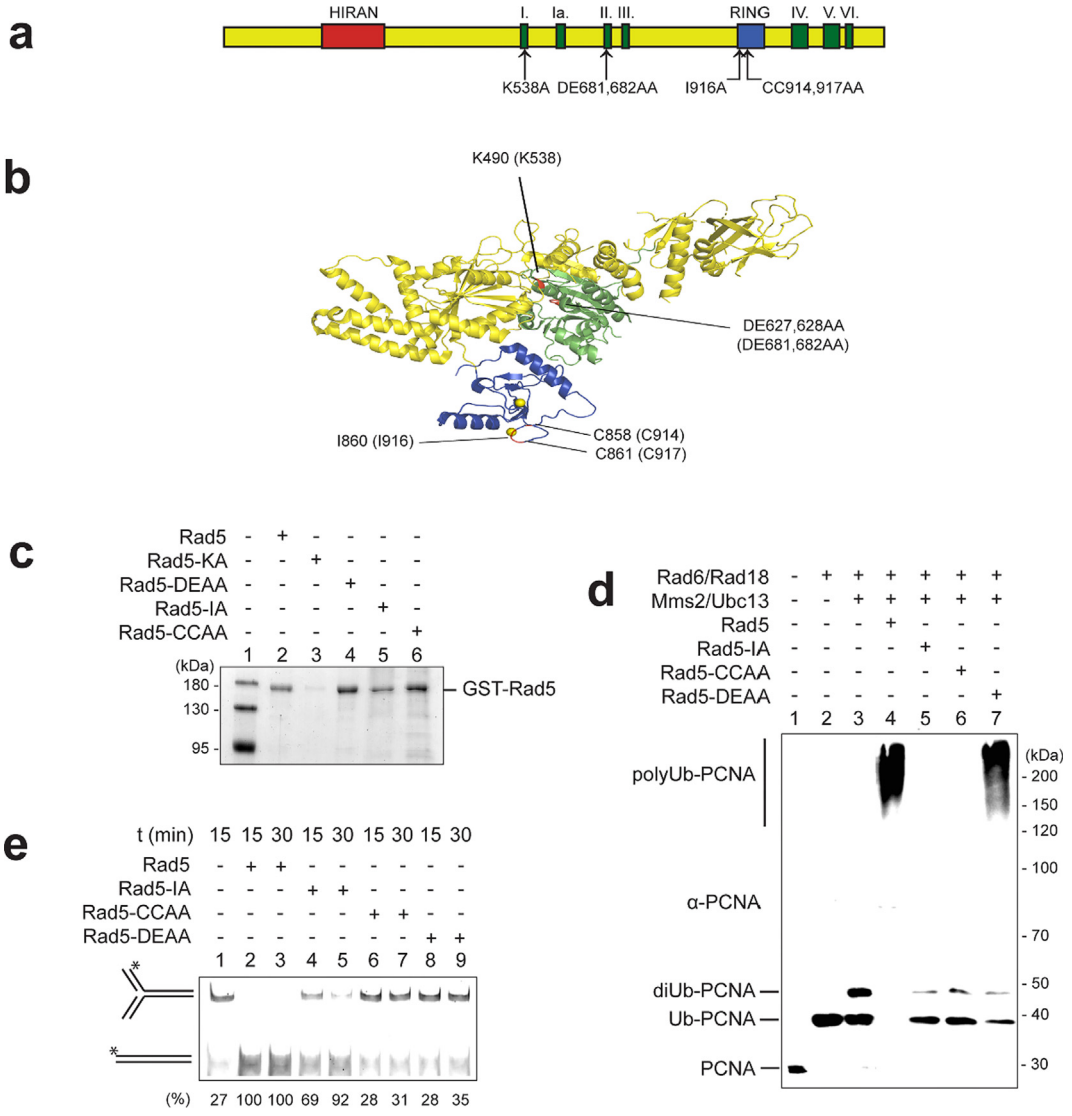

Figure 1. *In vitro* activities of recombinant Rad5 proteins. (A) Schematic representation of the domain structure of Rad5. The conserved motifs of the SWI2/SNF2 helicase domain are depicted as green boxes, the RING domain is indicated by a blue box, and the HIRAN domain is represented by a red box. The positions of the mutations generated are indicated by arrows. (B) The positions of the corresponding mutations in the crystal structure of *Kluyveromyces lactis* Rad5. *Sc*Rad5 amino acid numbers are in brackets. The RING domain is shown in blue, and the lobe 1 of the helicase domain in green. (C) Purity of the wild-type and mutant Rad5 protein samples (10 μl each). (D) PCNA polyubiquitylation by purified Rad5 proteins. The activity of wild-type and mutant Rad5 was assayed in the presence of Rad6/Rad18 and Mms2/Ubc13. Ub-PCNA: monoubiquitin-PCNA, PolyUb-PCNA: polyubiquitylated PCNA. (E) The dsDNA translocase activity of Rad5 proteins was tested using a fluorescently labeled oligonucleotide-based replication fork-like structure, which could be converted into a linear heteroduplex by Rad5. Schematic structures of the substrate and the product are shown on the left. Percentages of the remodeled linear heteroduplex formed after 15 and 30 minutes, as indicated, are given at the bottom. The linear heteroduplex detected in the first lane represents spontaneous realignment during the extended incubation.

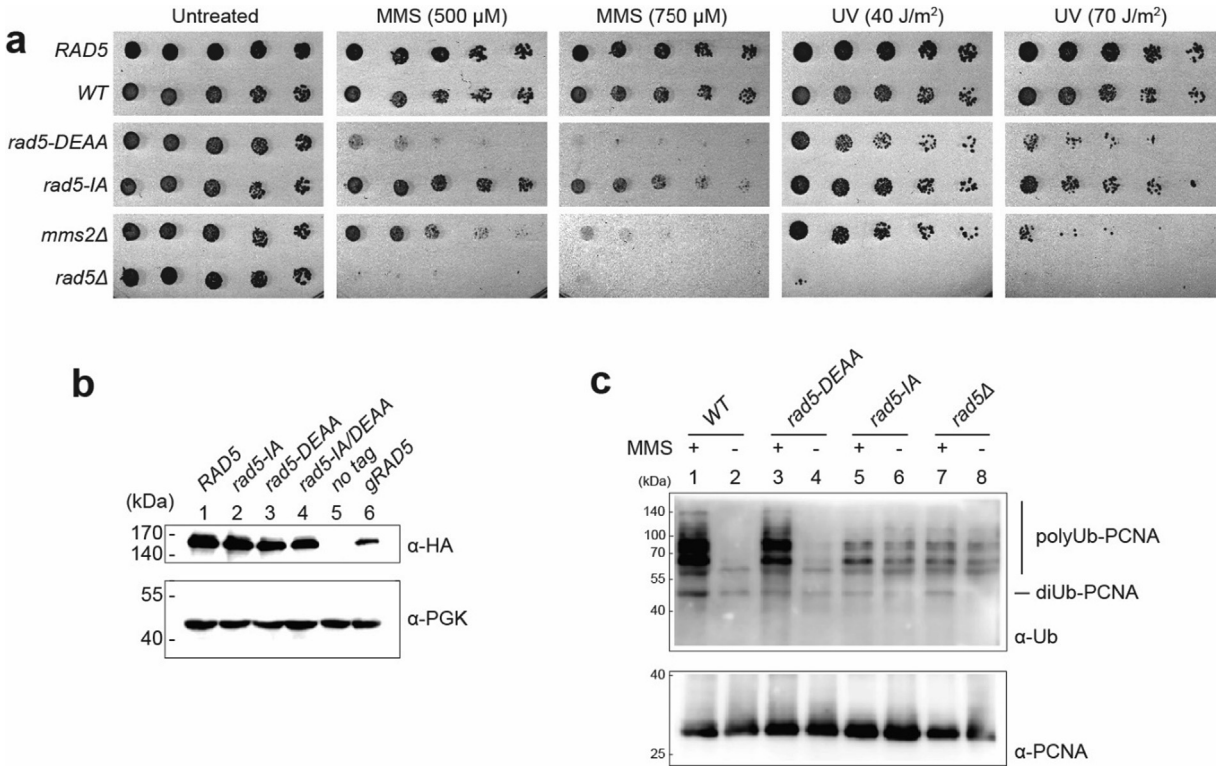

Figure 2. *In vivo* characterization of *rad5-IA* and *rad5-DEAA*. (A) DNA damage sensitivity of strains expressing wild-type or mutant Rad5. All strains were generated by transforming *rad5*Δ with an empty vector, or with plasmids expressing wild-type or mutant Rad5. Serial dilutions of the strains were spotted on plates containing the indicated doses of MMS or were UV-irradiated with the indicated UV doses after spotting. (B) The intracellular level of ectopically expressed HA-tagged Rad5 proteins was examined in whole-cell extracts by immunoblotting using anti-HA antibody. PGK served as a loading control, showed at the bottom. (C) MMS-induced PCNA polyubiquitylation was tested in *rad5* strains expressing 7His-PCNA from a plasmid. Cells were synchronized in G1 by α-factor prior to MMS treatment. Ubiquitylated forms of PCNA from whole-cell extracts were bound to Ni-beads and immunoblotted using an anti-ubiquitin antibody (upper panel). We note, that this antibody does not recognize the monoubiquitylated form of PCNA, as reported earlier by others and us.[2,56] Unmodified PCNA in the bound fraction was also detected by applying an anti-PCNA antibody on the lower part of the same membrane (lower panel).

interaction with Ubc13. In *rad5-CCAA*, the structure of the RING domain was disrupted by replacing two of its metal coordinating cysteines by alanine at positions 914 and 917, whereas the *rad5-IA* mutant carried a more subtle change at isoleucine-916 that still hindered the interaction with Ubc13.[35] The complete sequence of the alleles was verified by sequencing.

In vitro PCNA polyubiquitylation by mutant Rad5 proteins

To corroborate that the mutations selectively inactivated the corresponding domains, we overexpressed and purified the wild-type and mutant proteins from yeasts and examined their ubiquitin ligase and DNA remodeling activities in parallel, in well established *in vitro* systems. However, the yield of the Rad5-KA protein proved to be very low after purification in repeated attempts. Since the intracellular level of another ATP-binding motif mutant with the GKT/GAA changes was shown to be significantly decreased compared to the wild type, we surmised that altering lysine-538 could affect the stability or the folding of Rad5.[22] Since the low concentration of the purified protein hindered its investigation in *in vitro* enzymatic assays, it was omitted from further investigation (Figure 1(C)). The ability of Rad5 proteins to support PCNA polyubiquitylation was assessed using untagged PCNA that was first loaded onto DNA by the clamp loader replication factor C (RFC). Subsequently, enzymes needed for the mono- and polyubiquitylation steps were added to the reactions. As expected, the RING domain mutant Rad5-CCAA and Rad5-IA proteins were completely defective in PCNA polyubiquitylation (Figure 1(D)). We note, that the small amount of diubiquitylated PCNA detected in the reactions was produced by the Mms2/Ubc13 complex, as they were observed even in the absence of Rad5 (Figure 1(D), compare lane 3 to 5 and 6), and also

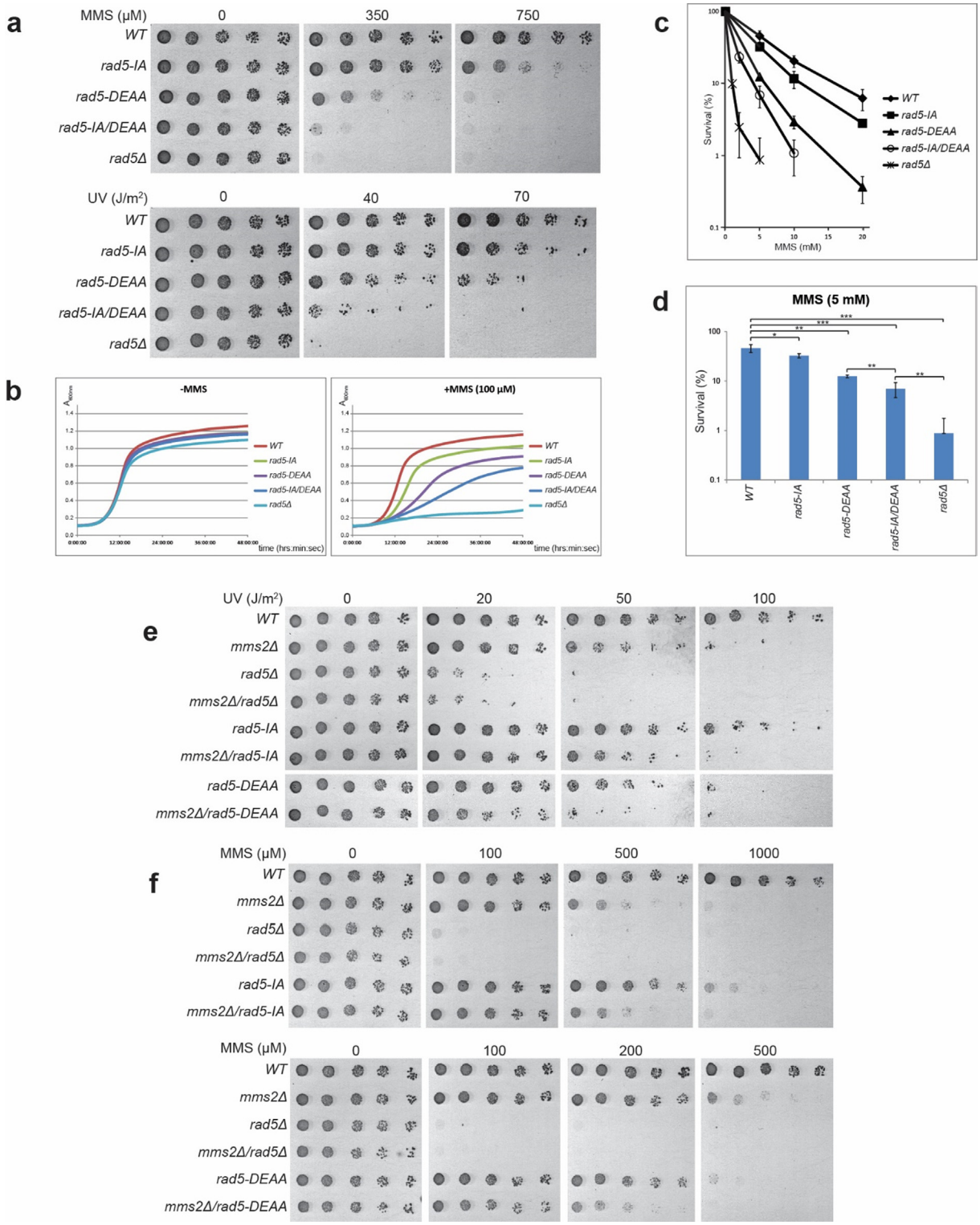

Figure 3. Genetic interactions of *rad5* mutants. The *rad5-IA/DEAA* is more sensitive to UV and MMS than the single mutants as shown using (A) serial dilution spot assay (B) growth curve assay with MMS-containing medium (C) killing curve by colony-counting plate assay. For (B), cultures containing ~50 cells were grown for 48 hours, and A_{600} was recorded with 4 min intervals. For (C) logarithmic cultures were treated with increasing concentration of MMS for 1 hour at 30 °C before plating. Colonies were counted after incubation for 3 days at 30 °C. The graph shows data of 3 independent experiments with standard deviations**.** (D) Results of the killing curve analysis shown in Fig. 3C at 5 mM MMS concentration depicted in a graph. P-values were calculated by Student t-test. *: p < 0,05, **: p < 0,01, ***: p < 0,001. **(**E,F**)** *rad5-IA* is epistatic, whereas *rad5-DEAA* is additive with *mms2*. Epistasis analysis of the given strains was done using serial dilution spot assay after (E) UV and (F) MMS treatment.

shown previously by us and others.[27,36] Most importantly, the ATPase mutant Rad5-DEAA exhibited almost as strong ubiquitin ligase activity as the wild type (Figure 1(D), compare lanes 4 and 7). This implies, that the DE681,682AA mutation slightly affects, though certainly does not destroy the ubiquitin ligase activity of Rad5. Since even *in vitro* PCNA polyubiquitylation requires the Rad5-Ubc13 interaction evidenced by the inactivity of Rad5-IA in these assays, we infer that the Walker B motif of the helicase domain is not necessary for the Rad5-Ubc13 interaction, contrary to previous suggestions by others.[24,25]

In vitro DNA remodeling activity of mutant Rad5 proteins

The functionality of the helicase domain was assessed by monitoring the DNA remodeling activity of Rad5 using a double-stranded branched DNA substrate mimicking a replication fork (Figure 1(E)). We have previously shown that wild-type Rad5 could easily remodel such a substrate into a double-stranded linear form in an ATP-hydrolysis-dependent manner.[20] Indeed, the wild-type and the Rad5-IA proteins were able to remodel the substrate DNA, though Rad5-IA showed somewhat lower activity. In contrast, the Rad5-DEAA ATPase mutant was completely inactive in these assays, in agreement with our previous results.[20] Interestingly, Rad5-CCAA was as defective as the ATPase mutant indicating that the CC914,917AA RING mutations inactivated not only the RING but the helicase domain, as well. The special arrangement of the two domains suggested that the mutations caused structural perturbation in the RING domain, which probably affected the surrounding helicase domain as well, leading to the inactivation of both domains. During this project, the crystal structure of a nearly full-length Rad5 of the yeast *Kluyveromyces lactis* (*Kl.*) showing 46.7% sequence identity with *Sc.*Rad5 was published, which revealed that though the RING domain is embedded in the helicase domain at the level of the amino acid sequence, protein folding separates the two domains in the three-dimensional structure (Figure 1(B)).[37] Nevertheless, because of the inactivity of its both domains, this mutant was not investigated further. In summary, the results of the *in vitro* enzymatic tests indicate that the I916A mutation compromises entirely the ubiquitin ligase, whereas the DE681,682AA the ATPase-linked activity, and they have only a slight effect on the other domain's activity: consequently, they can be considered domain-specific.

PCNA polyubiquitylation in the rad5-IA and rad5-DEAA strains

To investigate the *in vivo* effects of the mutations, we constructed yeast strains lacking the chromosomal copy of *RAD5* and ectopically expressing the wild-type or the mutant Rad5 proteins from a single copy plasmid under the regulation of the endogenous *RAD5* promoter and terminator sequences. Importantly, ectopically expressed wild-type *RAD5* conferred UV and MMS resistance to yeasts to the same degree as the chromosomal copy of the gene, whereas the mutants caused moderate sensitivities (Figure 2(A)). Since the expression levels of plasmid-born Rad5 proteins detected in whole-cell lysates were similar to each other and they were not lower than the level of endogenous Rad5, we concluded that the sensitivities were caused by the specific mutations, confirming that both the RING and the helicase domains contributed to Rad5 function (Figure 2(B)). We note that the *rad5-DEAA* strain exhibited much higher sensitivity to MMS than the *rad5-IA*, whereas there was considerably smaller difference between the UV sensitivities of the two strains (Figure 2(A)). That might indicate a more substantial role for the Rad5 helicase domain in the bypass of MMS-induced DNA damage. Using these strains, we tested PCNA polyubiquitylation, the best characterized *in vivo* task of Rad5, to assess whether the ubiquitin ligase activity of the mutants observed *in vitro* was also reflected *in vivo*. To facilitate detection, PCNA was expressed ectopically in fusion with a 7-histidine tag, and this 7His-PCNA construct served as a sole source of PCNA in cells lacking the chromosomal copy of the gene. Importantly, as Figure 2(C) shows, PCNA polyubiquitylation in the *rad5-DEAA* strain was proficient after MMS-treatment, though a small reduction in the amount of polyubiquitylated PCNA could be observed compared to the wild type, in accord with the *in vitro* activity of Rad5-DEAA as a ubiquitin ligase for PCNA. This raised the possibility that a small defect in PCNA polyubiquitylation caused by the DE/AA mutations contributed to the higher UV and MMS sensitivity of *rad5-DEAA* compared to *rad5-IA*. As expected, MMS-induced PCNA polyubiquitylation could not be detected in *rad5-IA* paralleling the inactivity of the corresponding mutant protein in the *in vitro* assay. Taken together, these results suggest that the selected mutations exert the same effects on Rad5 activity *in vitro* and *in vivo*, as well.

The ubiquitin ligase and ATPase-linked activities of Rad5 promote separate functions

Notably, the above experiments demonstrated that the ATPase-linked activity of Rad5 was dispensable for PCNA polyubiquitylation, suggesting that the ATPase-linked and the ubiquitin ligase activities of Rad5 participated in different steps of DNA damage bypass. To corroborate this, we created a *rad5-IA/DEAA* double mutant strain carrying mutations in both the RING and the helicase domains of Rad5 and compared its sensitivity to the single domain

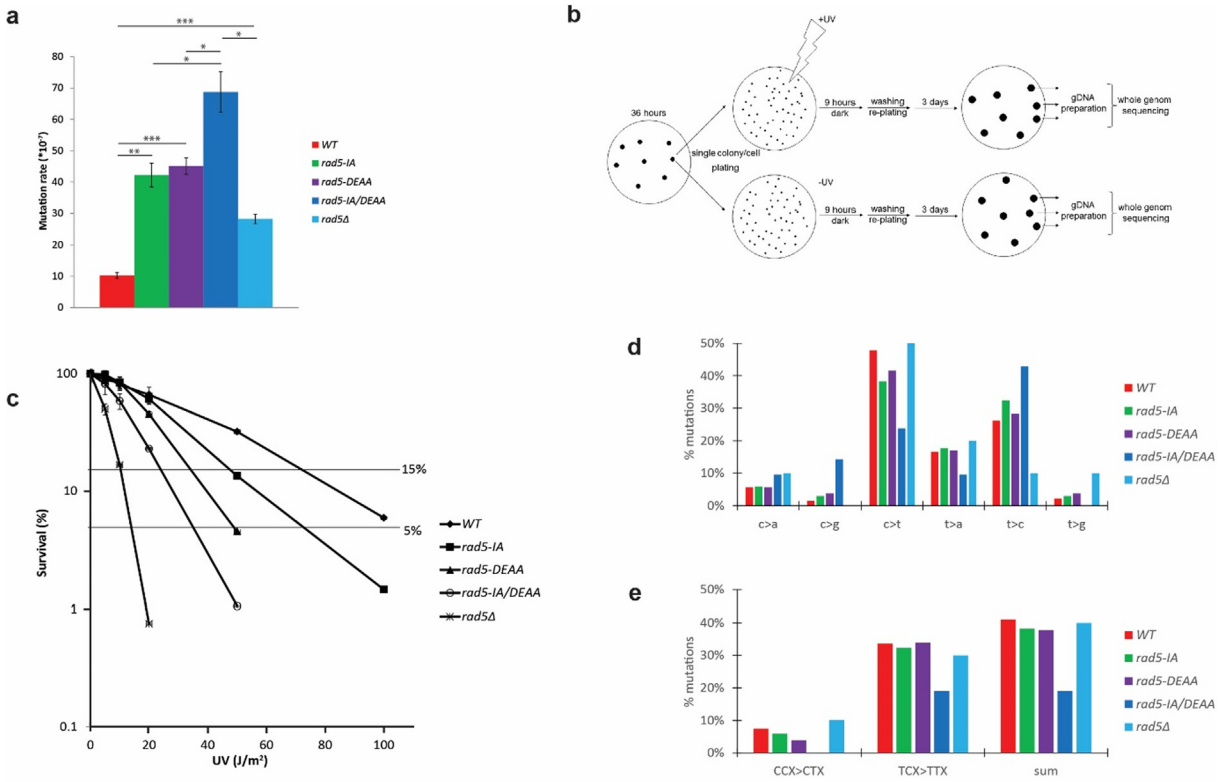

Figure 4. The effect of the RING and helicase mutations of *RAD5* on mutagenesis. (A) Spontaneous forward mutagenesis assay with *rad5* mutant strains. Canavanine resistant colonies were counted and calculated for 10^7 surviving cells. The graph represents the average of 5 independent experiments. Standard deviations are shown. (B) Flowchart of sample processing for whole-genome sequencing. (C) UV killing curve of the indicated strains to determine the UV doses necessary to obtain ~10% survival before collecting cells for whole-genome sequencing. (D) Mutation signature analysis of UV-treated *rad5* mutant strains. The frequencies of 6 categories of mutations are represented. (E) C > T mutations occur primarily at the 3′ C of TC dipyrimidines.

mutants after treating the cells with UV or MMS. As Figure 3(A)–(D) shows, the double mutant exhibited significantly higher sensitivity than the single mutants in different assays, indicating independent roles for the RING and helicase domains. These results were confirmed in experiments investigating the genetic relations of the domain-specific *rad5* mutants to *mms2*Δ. Epistasis analysis showed that the *mms2*Δ *rad5-IA* double mutant strain exhibited the same sensitivity to UV and MMS as the *mms2*Δ single mutant, suggesting that the ubiquitin ligase activity of Rad5 works exclusively in connection with Mms2 (Figures 3(E) and (F)). Contrary to that, the *mms2*Δ *rad5-DEAA* double mutant strain was more sensitive than the corresponding single mutants. Similar results were obtained in the *ubc*13Δ background (Figure S1) Taken together, our findings underpin an Mms2- and PCNA polyubiquitylation-independent contribution of the helicase domain of Rad5 to DNA damage bypass. These results correspond well with the spatial separation of the RING and helicase domains in the crystal structure of *Kl*.Rad5 suggesting independent functions to the domains. We note though, that our results do not exclude the possibility that the helicase domain also contributes to the *MMS2*-dependent pathway, together with the RING domain. However, the role of the helicase domain must be sequential to PCNA polyubiquitylation and is most probably catalytic.

The effect of domain-specific Rad5 mutants on spontaneous mutagenesis

A characteristic of *rad*5Δ strains is the increased rate of spontaneous mutagenesis, indicating that the function of Rad5 is mainly error-free.[38,39] To test the contribution of the ubiquitin ligase and the ATPase-linked activities to the error-free function, we examined the effect of the domain-specific mutants on spontaneous mutagenesis. Using the canavanine mutagenesis reporter assay we found that spontaneous mutagenesis was equally elevated in the *rad5-IA* and in the *rad5-DEAA* mutant

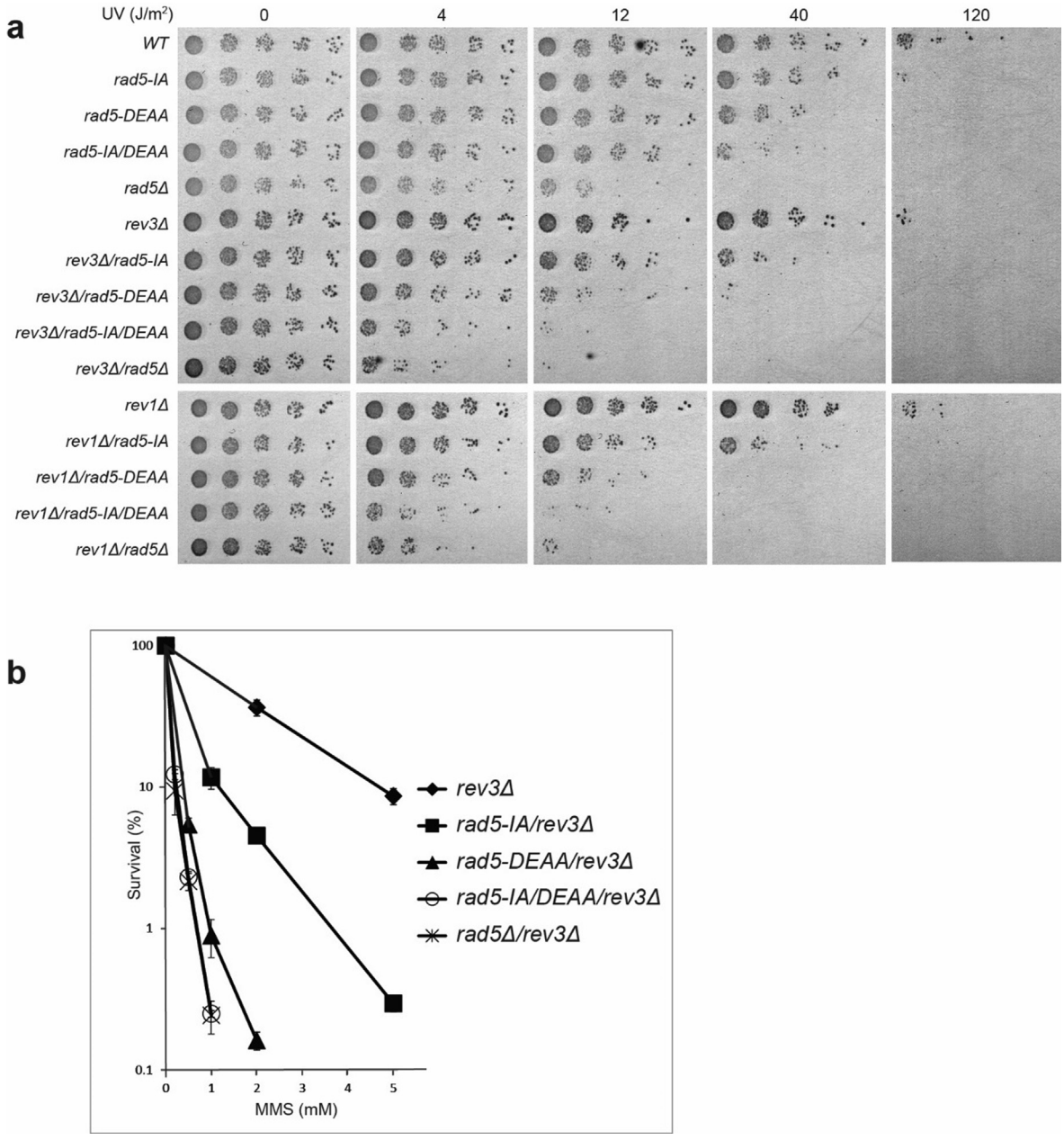

Figure 5. Epistasis analysis of *rad5* mutants with *rev*3Δ and *rev*1Δ. (A) A serial dilution assay using increasing UV doses. (B) Genetic relation of *rev*3Δ and *rad5* mutants examined after MMS treatment. The graph represents data from 3 independent colony-counting plate assays. Cells were treated with increasing concentrations of MMS and spread onto plates. Colonies were counted after 3 days of incubation at 30 °C. Standard deviations are also shown.

strains exhibiting a more than four times higher mutation rate compared to the wild type. These data suggested that both the ubiquitin ligase and ATPase-linked activities of Rad5 had error-free roles under physiological conditions (Figure 4(A)). Importantly, in the double domain mutant *rad5-IA/DEAA* strain the rate of spontaneous mutagenesis was ∼1.5 times higher than the rate measured in the single mutants pointing to independent error-free functions of the ubiquitin ligase and the ATPase-linked activities of Rad5. It is noteworthy, that the mutation rate of the *rad*5Δ strain is lower than that of the single and double mutant strains but still higher than that of the wild type, indicating that Rad5 has a pro-mutagenic function that is independent of its ubiquitin ligase and ATPase-linked activities.

Rad5 exerts its roles via three activities during DNA damage tolerance

Indeed, in addition to its role in error-free DDT, Rad5 was shown to support error-prone bypass of the DNA lesions by TLS DNA polymerases through its interaction with Rev1.[40,41] The above experiments showed that the UV and MMS sensitivities of the double domain mutant *rad5-IA/DEAA* strain were lower than that of *rad5*Δ and that spontaneous mutagenesis in *rad5-IA/DEAA* was significantly higher than in the *rad5*Δ strain in agreement with a mutagenic, non-catalytic role for Rad5 in damage bypass. To obtain additional evidence, we carried out epistasis analysis with prominent members of the mutagenic TLS pathway. In line with the above results, our genetic analysis showed that the sensitivity of the *rad5-IA* and the *rad5-DEAA* strains and also of the double domain mutant *rad5-IA/DEAA* to UV and MMS was greatly increased by deleting *REV3* or *REV1*, confirming that the catalytic activities of the RING and the helicase domains of Rad5 did not contribute to mutagenic TLS (Figures 5 and S2). Importantly, the equal UV and MMS sensitivity of the *rev3*Δ *rad5-IA/DEAA*, the *rev1*Δ *rad5-IA/DEAA*, the *rev3*Δ *rad5*Δ, and the *rev1*Δ *rad5*Δ strains indicated that deletion of *REV3* or *REV1* completely inhibited the RING and helicase domain-independent function of Rad5. This implies that besides the RING and helicase domain-associated catalytic functions, the remaining role of Rad5 is exerted together with Rev1 and Rev3 in error-prone TLS. In this study, we did not investigate the HIRAN domain found at the N-terminus in Rad5 and HLTF because of its involvement in the different functions of Rad5.[42] The HIRAN domain is a highly conserved DNA-binding domain that contributes to both the ubiquitin ligase and the ATPase-linked functions, as it was shown to be necessary for full activity of HLTF during PCNA polyubiquitylation and for fork reversal by HLTF and Rad5 as well.[43–47] A critical role of the HIRAN domain of *Kl*. Rad5 in PCNA polyubiquitylation and replication fork regression was also reported.[37]

Table 1 Plasmids used in the study.

Number	RAD5	Vector
pIL101	*WT*	pBJ842
pIL102	*CC914,917AA*	pBJ842
pIL667	*K538A*	pBJ842
pIL668	*DE681,682AA*	pBJ842
pIL2780	*I916A*	pBJ842
pID178	*WT*	YCplac111
pID180	*DE681,682AA*	YCplac111
pID565	*empty*	YCplac111
pID745	*I916A*	YCplac111
pID1180	*I916A,DE681,682AA*	YCplac111
pID1243	*7His-PCNA*	YCplac33

UV-induced mutational spectrum of rad5 domain-specific mutants

Mutational spectrum is characteristic of enzymes responsible for generating them. Therefore, we planned to identify mutations in *rad5* strains to obtain information on the proteins activated in the absence of specific Rad5 functions. However, instead of relying on reporter genes, we sequenced the entire genome by next-generation sequencing to attain a more unbiased picture (Figure 4(B)). To enrich for mutations, we treated cells with different UV doses to obtain ∼10% survival, before determining the single nucleotide mutation spectrum of each strain (Figure 4(C)). Curiously, as Figure 4(D) shows, the mutation pattern was similar in the wild-type and the single mutant *rad5-IA* and *rad5-DEAA* cells; however, striking differences could be detected in the double domain mutant *rad5-IA/DEAA* samples. First, the ratio of C > T mutations dropped from ∼40% in the wild type and the single mutants to ∼20%, moreover, those of the C > G and the T > C mutations increased from 2-3% to ∼17%, and from ∼30% to ∼40%, respectively, in the double mutant. The C > T mutation is a UV signature mutation that most commonly forms at the 3′ C of TC and CC pyrimidine dimers.[48] The reason behind this is that UV induces the deamination of cytosines, and cytosines in dimers are more unstable than in a normal sequence. Indeed, we found that C > T was the most prevalent change accounting for ∼40% of all mutations in the wild type and the single mutants, and ∼90% of them occurred at the 3′ C of dipyrimidine sites (Figure 4(E)). In *Escherichia coli*, C > T mutations were proposed to mainly result from error-free insertion of adenine opposite the uracil in place of the spontaneously deaminated 3′ C of the dimer.[49] In humans, error-free bypass of deaminated dimers by Polη was suggested, but the observation that in cells having a defective Polη C > T transition is still the most prominent UV-induced mutation argues against it.[50,51] Genetic studies in yeast did not support a role for Polη in generating C > T transitions either, instead, they provided evidence for an essential role of Rev3.[52] In light of that, it is puzzling that inactivation of the error-free functions of Rad5 in *rad5-IA/DEAA* decreases the incidence of a mutagenic event. All the more because the ratio of C > T mutations goes back to the wild type level in the absence of Rad5. C > G transversions at dipyrimidines are proposed to result from error-prone insertion of C opposite abasic sites by Rev1, which arise after the removal of uracil formed by deamination of the 3′ C in the dimers.[10] Since C > G transversions in *rad5-IA* and *rad5-DEAA* cells occur at Cs between two pyrimidines, it is unclear whether the mutations were formed at the 5′ or 3′ bases. In addition, in *rad5-IA/DEAA* C > G mutations are detected at the 5′ C of dipyrimidines as well, suggesting that error-prone insertion opposite the 5′ C of the

dimers, probably by Rev1, also contributes to C > G transversions. The proportion of T > C inversions also increased by more than 10% in *rad5-IA/DEAA* cells. Surprisingly, our data suggest that, despite its role in mutagenesis, the absence of Rad5 results only in minor perturbation in the activation of the mutagenic pathways. The only major difference identified between the spectrums of base substitutions in wild-type and *rad5*Δ cells is the strongly reduced ratio of T > C inversions, which dropped from ~30% in the wild type to 10% in *rad5*Δ. This finding correlates well with data showing that T > C mutations resulting from translesion synthesis opposite (6–4) TT photoproducts in yeasts almost entirely depend on *RAD5*.[53] Taken together, these results further confirm an independent function of the Rad5 RING and helicase domains and they reveal that concurrent inactivation of the two domains alters the activation of the mutagenic pathways. Based on these findings, we infer that in wild-type cells the mutagenic pathway relies on the catalytic activity of Rev3. However, when error-free damage bypass by Rad5 is impaired, the catalytic contribution of Rev1, which is marginal in the wild type and the single mutants, becomes significant, and this pathway depends on a non-enzymatic contribution of Rad5.

In summary, the results we obtained applying different assays are congruent and they establish that the contribution of both the helicase and the RING domains to error-free damage bypass requires their catalytic activities, which can work independently of each other**,** and during bypass they can support separate functions. Moreover, we can also conclude that Rad5 has only one additional role, a non-enzymatic contribution to mutagenic translesion synthesis, where it plays a dominant role during damage bypass catalyzed by Rev1 (Figure 6). Future studies aiming at exploring the interplay between selected activities of the multifunctional Rad5 and other proteins of DDT are needed to reveal the full spectrum of influence that Rad5/HLTF/SHPRH exert on genome stability.

Material and Methods

Yeast strains

Single deletion mutants in BY4741 and BY4742 background (EUROSCARF) were applied in the genetic studies. Double mutants were made by crossing, and deletions were confirmed by PCR. For the rescue of *rad5*Δ, strains were transformed with wild-type or mutant Rad5-expressing plasmids and maintained on synthetic dropout (SD) medium lacking leucine (-leu) to select for the plasmids. The BJ5464 strain was used for overexpressing Rad5 proteins. Spontaneous forward mutation frequencies at the *CAN1* locus were measured in EMY74.7 background. PCNA ubiquitylation was assayed in DF5a derivatives[54] expressing 7His-PCNA and the Rad5 proteins from centromeric plasmids.

Plasmids

Constructs used in this study are listed in Table 1. For rescue assays, the genomic *RAD5* PstI-SalI fragment containing promoter (339 bp) and terminator (623 bp) sequences were cloned into the centromeric low-copy plasmid YCplac111. Point mutations were generated in this plasmid via site-specific PCR mutagenesis and were verified by sequencing. The wild-type and the mutant *RAD5* genes were C-terminally tagged with six copies of the hemagglutinin epitope tag (6-HA) in the YCplac111 vector.[55] For the purification of the mutant Rad5 proteins, the point mutant and wild-type *RAD5* ORFs were first cloned into Gateway® entry vector (pENTR™) followed by recombination into destination plasmid (pBJ842 backbone), from which Rad5 was expressed in fusion with an N-terminal glutathione-S-transferase (GST) tag, under the control of a modified galactose-inducible phosphoglycerate kinase (*PGK*) promoter. The 7His-PCNA, with its promoter and terminator sequences, was cloned into the centromeric low-copy plasmid YCplac33.[56]

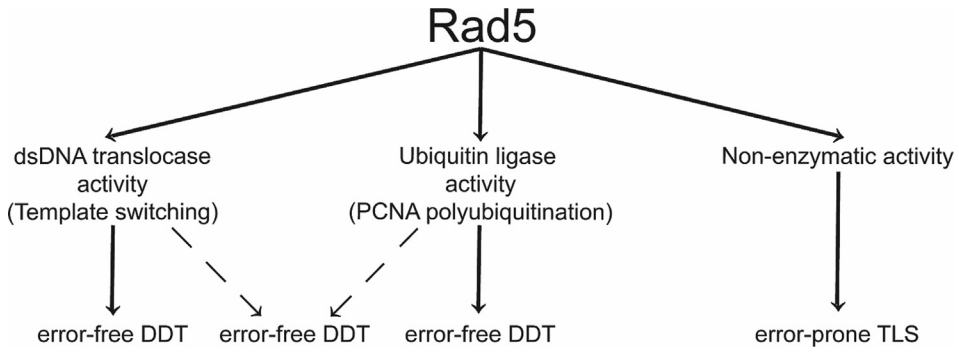

Figure 6. Contribution of Rad5 to DDT. Arrows with dashed lines indicate a putative error-free pathway involving both the helicase and RING domain-linked activities of Rad5.

Yeast sensitivity assays

For qualitative serial dilution assays, cells were grown in SD-leu to A_{600}:0.6, counted, and cell number was adjusted to 5×10^6 cells/ml. Dilutions were prepared in 3× steps and spotted onto SD-leu plates containing different amounts of MMS. For UV treatment, dilutions were spotted onto SD-leu plates and then UV-irradiated. Plates were scanned after 2–4 days of incubation in the dark at 30 °C.

For quantitative colony-counting plate assays, yeasts were grown to A_{600}:0.6, cells were counted, and cultures were diluted to 10^7 cells/ml and incubated by shaking for 1 hour at 30 °C in SD-leu containing different concentrations of MMS. After washing, appropriate dilutions were made and cells were spread onto SD-leu plates. Plates were incubated for 3 days at 30 °C before colonies were counted.

For growth curve assays, yeast strains were grown at 30 °C for 16 hours, and approximately 50 cells from each strain were inoculated into 500 μl SD-leu with or without 100 μM MMS. Plates were shaken at 30 °C in Synergy 2 Multi-Mode Reader (BioTek®), and A_{600} was measured every 4 minutes for 48 hours. Growth curves were determined using Microsoft® Excel 2010.

Spontaneous mutagenesis

Seven parallel cultures of approximately 50 cells each were grown in SD-leu for 2 days at 30 °C. The cultures were plated onto canavanine-containing SD-leu/-arg plates, and the median number of mutants in the case of each strain was counted for 10^7 plated cells. Mutation frequencies were determined using a chart based on the Lea-Coulson fluctuation model.[57] Results are averages of 5 independent experiments.

Whole-genome sequencing

A single colony from each strain was picked and dispersed in PBS and spread onto two SD-leu plates of which one was irradiated with UV. Different UV dosages were used to get ~10% survival with each strain (*WT*: 100 J/m^2, *rad5-IA*: 60 J/m^2, *rad5-DEAA*: 40 J/m^2, *rad5-IA/DEAA*: 30 J/m^2, *rad5*Δ:13 J/m^2). After 9-hour incubation at 30 °C in the dark, cells were collected from plates with PBS and were spread onto fresh SD-leu plates. Following a 3-day incubation at 30 °C, genomic DNA was extracted by phenol–chloroform from 3 colonies/samples, and the 3 parallel DNA samples were pooled. With the *rad5*Δ strain, the UV treatment and incubation steps were repeated 5 times using 3 single colonies. For whole-genome sequencing, the library was made with Nextera XT Library Preparation Kit (Cat.no. FC-131–1024, Illumina). For obtaining 2 × 150 bp paired-end sequence reads, Illumina NextSeq 500 sequencer was used. The average sequencing coverage was 100. Reads were aligned to the GCA_000146045.2 reference genome using BWA mem.[58] SAM files have been transformed to BAM and indexed with SAMtools.[59] Sequencing duplicates were removed using GATK MarkDuplicates.[60] Variants have been identified with freebayes using --min-base-quality 28 command and filtered with Vcflib using vcffilter tool and -f 'QUAL > 100′ setting.[61] Sample pairs have been compared by selecting only those variants which were not present, or their frequency was below 10% in untreated samples and over 60% or 20% in single or mixed samples, respectively. Data produced by whole genome sequencing is available at NCBI Genome Data Viewer (https://dataview.ncbi.nlm.nih.gov/object/PRJNA726574?reviewer=3ak2c50vp52g91hon6gj7dps78)

Protein purification

GST-Rad5 expression in BJ5464 was induced with 2% galactose for 8 hours followed by purification on glutathione-Sepharose beads. Bound proteins were eluted with 25 mM reduced glutathione as described previously.[34]

In vitro enzymatic assays

For helicase assays, reactions contained 20 mM Tris/HCl pH:7.0, 5 mM $MgCl_2$, 100 μg/ml bovine serum albumin (BSA), 1 mM dithiothreitol (DTT), 10% glycerol, and 5 mM ATP with 20 nM Rad5 proteins. Fluorescently labelled oligonucleotide (O3063: [Fluorescein]-GTTTTCCCAGTCACGACG ATGCTCCG

GTACTCCAGTGTAGGCATATTACGAATTCTT GAGGCAGGCATGGTAGCT) was used to produce a replication fork model substrate with hybridization to O1054 (AGCTACCATGCCTGCC TCAAGAATTCG

TAA), followed by hybridization to O3085 (AGCT ACCATGCCTGCCTCAAGAATTCGTAATATGCC TAC

ACTGGAGTACCGGAGCATCGTCGTGACTGG GAAAAC) - O1056 (TTACGAATTCTTGAGGCA GGCA

TGGTAGCT) dimer oligonucleotides. After 15 and 30 min incubation at 30 °C, samples were run on native PAGE (containing 2.5% glycerol and 0.5xTB). The gel was visualized with a Typhoon TRIO imager.

PCNA ubiquitylation reactions were carried out in a buffer containing 30 mM Tris-HCl pH:7.5, 5.5 mM $MgCl_2$, 7 μg/ml BSA, 7% glycerol, and 0.5 mM ATP. Purified ubiquitin (50 μM), PCNA (50 nM), RFC (10 nM), Uba1 (100 nM), Rad6/Rad18 (100 nM), Mms2/Ubc13 (100 nM), and Rad5 (20 nM) proteins were used in the reactions with 10 ng/μl BstNBI-nicked pUC19 plasmid DNA for PCNA loading. After 60-min incubation at 30 °C, samples were run on SDS-PAGE and immunoblotted with

anti-PCNA primary (1000×, Abcam 5E6/2) and anti-mouse secondary antibody (10 000×, Thermo Scientific 31430).

Whole-cell extract preparation and Ni-NTA chromatography

In vivo PCNA ubiquitylation was tested by denaturing Ni-nitriloacetic acid (Ni-NTA) chromatography.[62] Briefly, 200–200 ml of cell cultures expressing wild-type or mutant Rad5 and 7His-PCNA were grown in SC-leu medium. At A_{600}:0.8, cells were synchronized in G1 by α-factor for 3.5 h, then half of the cultures were treated with 0.02% MMS for 90 min. Whole-cell extracts were prepared by lysing cells in 0.24 M NaOH, 1% 2-mercaptoethanol (2-ME) for 15 min on ice. Proteins were precipitated by adding trichloroacetic acid to 6% and further incubation on ice for 10 min. After collection, precipitated proteins were solubilized in buffer A (10 mM Tris/HCl pH:8.0, 100 mM sodium-phosphate buffer pH:8.0, 6 M guanidyl-HCl) for 1 h at room temperature (RT). Clarified lysates were adjusted to pH:8.0 and supplemented with 10 mM imidazole and 0.05% Tween-20 before adding to 30 μl of Ni-NTA beads. Samples were incubated at RT overnight on a rotator. The next day, beads were collected and washed two times in buffer A and three times in buffer B (10 mM Tris/HCl pH:8.0, 100 mM sodium-phosphate buffer pH:8.0, and 8 M urea). Bound proteins were eluted by incubating the Ni-beads for 10 minutes at 60 °C in 20 μl of HU buffer (8 M urea, 200 mM Tris/HCl, pH:6.8, 1 mM EDTA, 5% SDS, 0.1% bromophenol blue, and 1.5% DTT). Samples were run on a 10% SDS PAGE and transferred onto a PVDF membrane (Immobilon-P, Merck Millipore Ltd.). Before probing with antibodies, membranes were pretreated either in 6 M guanidyl-HCl, 20 mM Tris/HCl pH:7.5, 5 mM 2-ME for 30 min at 4 °C for labeling with anti-Ub antibody (2000×, P4D1, Cell Signaling Technology) or 30 min at RT in stripping buffer (0.2 M glycine, 0.1% SDS, 1% Tween-20) for PCNA antibody (1000×, Abcam 5E6/2). For testing the expression level of HA-tagged mutant Rad5 proteins, whole-cell extracts prepared from 5 ml A_{600}:1 cultures were immunoblotted with anti-HA (10,000×, Abcam ab9110) and anti-PGK (10,000×, Molecular Probes A6457) primary, and anti-rabbit (10,000×, Thermo Scientific 31460) or anti-mouse (10,000× Thermo Scientific 31430) secondary antibodies, respectively.

CRediT authorship contribution statement

Robert Toth: Investigation, Validation, Visualization. **David Balogh:** Investigation. **Lajos Pinter:** Supervision, Software. **Gabor Jaksa:** Software. **Bence Szeplaki:** Software. **Alexandra Graf:** Investigation. **Zsuzsanna Gyorfy:** Investigation. **Marton Zs. Enyedi:** Investigation. **Erno Kiss:** Supervision, Visualization, Software. **Lajos Haracska:** Conceptualization, Funding acquisition, Writing – review & editing. **Ildiko Unk:** Conceptualization, Funding acquisition, Writing – original draft.

Acknowledgement

The authors thank Katalin Kovacs, Aniko Bozo-Toth, Szilvia Minorits, and Anita Nemeth for technical assistance, and Gabriella Tick for proofreading the manuscript.

Declaration of Competing Interest

The authors declare that they have no known competing financial interests or personal relationships that could have appeared to influence the work reported in this paper.

Appendix A. Supplementary data

Supplementary data to this article can be found online at https://doi.org/10.1016/j.jmb.2021.167437.

Received 15 September 2021;
Accepted 28 December 2021;
Available online 3 January 2022

Keywords:
Rad5;
DNA damage tolerance;
mutagenesis;
yeast genetics;
enzyme assay

† Joint last authors.

References

1. Torres-Ramos, C.A., Prakash, S., Prakash, L., (2002). Requirement of RAD5 and MMS2 for Postreplication Repair of UV-Damaged DNA in Saccharomyces cerevisiae. *Mol. Cell. Biol.* **22**, 2419–2426. https://doi.org/10.1128/mcb.22.7.2419-2426.2002.
2. Hoege, C., Pfander, B., Moldovan, G.-L., Pyrowolakis, G., Jentsch, S., (2002). RAD6-dependent DNA repair is linked to modification of PCNA by ubiquitin and SUMO. *Nature* **419**, 135–141. https://doi.org/10.1038/nature00991.
3. Stelter, P., Ulrich, H.D., (2003). Control of spontaneous and damage-induced mutagenesis by SUMO and ubiquitin conjugation. *Nature* **425**, 188–191. https://doi.org/10.1038/nature01965.
4. Prakash, S., Johnson, R.E., Prakash, L., (2005). Eukaryotic translesion synthesis DNA polymerases: specificity of structure and function. *Annu. Rev. Biochem.* **74**, 317–353. https://doi.org/10.1146/annurev.biochem.74.082803.133250.

5. McDonald, J.P., Levine, A.S., Woodgate, R., (1997). The Saccharomyces cerevisiae RAD30 gene, a homologue of Escherichia coli dinB and umuC, is DNA damage inducible and functions in a novel error-free postreplication repair mechanism. *Genetics.* **147**, 1557–1568 (accessed May 20, 2019) http://www.ncbi.nlm.nih.gov/pubmed/9409821.
6. Johnson, R.E., Prakash, S., Prakash, L., (1999). Efficient bypass of a thymine-thymine dimer by yeast DNA polymerase, Poleta. *Science* **283**, 1001–1004 (accessed May 20, 2019) http://www.ncbi.nlm.nih.gov/pubmed/9974380.
7. Nelson, J.R., Lawrence, C.W., Hinkle, D.C., (1996). Thymine-thymine dimer bypass by yeast DNA polymerase ζ. *Science (80-)* **272**, 1646–1649. https://doi.org/10.1126/science.272.5268.1646.
8. Haracska, L., Unk, I., Johnson, R.E., Johansson, E., Burgers, P.M.J., Prakash, S., Prakash, L., (2001). Roles of yeast DNA polymerases δ and ζ of Rev 1 in the bypass of abasic sites. *Genes Dev.* **15**, 945–954. https://doi.org/10.1101/gad.882301.
9. Johnson, R.E., Washington, M.T., Haracska, L., Prakash, S., Prakash, L., (2000). Eukaryotic polymerases iota and zeta act sequentially to bypass DNA lesions [In Process Citation]. *Nature* **406**, 1015–1019.
10. Nelson, J.R., Lawrence, C.W., Hinkle, D.C., (1996). Deoxycytidyl transferase activity of yeast REV1 protein. *Nature* **382**, 729–731. https://doi.org/10.1038/382729a0.
11. Haracska, L., Prakash, S., Prakash, L., (2002). Yeast Rev1 protein is a G template-specific DNA polymerase. *J. Biol. Chem.* **277**, 15546–15551. https://doi.org/10.1074/jbc.M112146200.
12. Daraba, A., Gali, V.K., Halmai, M., Haracska, L., Unk, I., (2014). Def1 promotes the degradation of Pol3 for Polymerase Exchange to Occur During DNA-Damage-Induced Mutagenesis in Saccharomyces cerevisiae. *PLoS Biol.* **12**, https://doi.org/10.1371/journal.pbio.1001771 e1001771.
13. Zhang, H., Lawrence, C.W., (2005). The error-free component of the RAD6/RAD18 DNA damage tolerance pathway of budding yeast employs sister-strand recombination. *Proc. Natl. Acad. Sci. USA* **102**, 15954–15959. https://doi.org/10.1073/pnas.0504586102.
14. Broomfield, S., Chow, B.L., Xiao, W., (1998). MMS2, encoding a ubiquitin-conjugating-enzyme-like protein, is a member of the yeast error-free postreplication repair pathway. *Proc. Natl. Acad. Sci. USA* **95**, 5678–5683. https://doi.org/10.1073/pnas.95.10.5678.
15. Ulrich, H.D., Jentsch, S., (2000). Two RING finger proteins mediate cooperation between ubiquitin-conjugating enzymes in DNA repair. *EMBO J.* **19**, 3388–3397. https://doi.org/10.1093/emboj/19.13.3388.
16. Brusky, J., Zhu, Y., Xiao, W., (2000). UBC13, a DNA-damage-inducible gene, is a member of the error-free postreplication repair pathway in Saccharomyces cerevisiae. *Curr. Genet.* **37**, 168–174 (accessed May 21, 2019) http://www.ncbi.nlm.nih.gov/pubmed/10794173.
17. Hofmann, R.M., Pickart, C.M., (1999). Noncanonical MMS2-Encoded Ubiquitin-Conjugating Enzyme Functions in Assembly of Novel Polyubiquitin Chains for DNA Repair. *Cell* **96**, 645–653. https://doi.org/10.1016/S0092-8674(00)80575-9.
18. Johnson, R.E., Henderson, S.T., Petes, T.D., Prakash, S., Bankmann, M., Prakash, L., (1992). Saccharomyces cerevisiae RAD5-encoded DNA repair protein contains DNA helicase and zinc-binding sequence motifs and affects the stability of simple repetitive sequences in the genome. *Mol. Cell. Biol.* **12**, 3807–3818. https://doi.org/10.1128/mcb.12.9.3807.
19. Johnson, R.E., Prakash, S., Prakash, L., (1994). Yeast DNA repair protein RAD5 that promotes instability of simple repetitive sequences is a DNA-dependent ATPase. *J. Biol. Chem.* **269**, 28259–28262. https://doi.org/10.1016/s0021-9258(18)46922-0.
20. Blastyák, A., Pintér, L., Unk, I., Prakash, L., Prakash, S., Haracska, L., (2007). Yeast Rad5 protein required for postreplication repair has a DNA helicase activity specific for replication fork regression. *Mol. Cell.* **28**, 167–175. https://doi.org/10.1016/j.molcel.2007.07.030.
21. Minca, E.C., Kowalski, D., (2010). Multiple Rad5 activities mediate sister chromatid recombination to bypass DNA damage at stalled replication forks. *Mol. Cell.* **38**, 649–661. https://doi.org/10.1016/j.molcel.2010.03.020.
22. Chen, S.S., Davies, A.A., Sagan, D., Ulrich, H.D., (2005). The RING finger ATPase Rad5p of Saccharomyces cerevisiae contributes to DNA double-strand break repair in a ubiquitin-independent manner. *Nucleic Acids Res.* **33**, 5878–5886. https://doi.org/10.1093/nar/gki902.
23. Ortiz-Bazán, M.Á., Gallo-Fernández, M., Saugar, I., Jiménez-Martín, A., Vázquez, M.V., Tercero, J.A., (2014). Rad5 plays a major role in the cellular response to DNA damage during chromosome replication. *Cell Rep.* **9**, 460–468. https://doi.org/10.1016/j.celrep.2014.09.005.
24. Ball, L.G., Xu, X., Blackwell, S., Hanna, M.D., Lambrecht, A.D., Xiao, W., (2014). The Rad5 helicase activity is dispensable for error-free DNA post-replication repair. *DNA Repair (Amst).* **16**, 74–83. https://doi.org/10.1016/j.dnarep.2014.02.016.
25. Choi, K., Batke, S., Szakal, B., Lowther, J., Hao, F., Sarangi, P., Branzei, D., Ulrich, H.D., et al., (2015). Concerted and differential actions of two enzymatic domains underlie Rad5 contributions to DNA damage tolerance. *Nucleic Acids Res.* **43**, 2666–2677. https://doi.org/10.1093/nar/gkv004.
26. Unk, I., Hajdú, I., Blastyák, A., Haracska, L., (2010). Role of yeast Rad5 and its human orthologs, HLTF and SHPRH in DNA damage tolerance. *DNA Repair (Amst).* **9**, 257–267. https://doi.org/10.1016/j.dnarep.2009.12.013.
27. Unk, I., Hajdú, I., Fátyol, K., Szakál, B., Blastyák, A., Bermudez, V., Hurwitz, J., Prakash, L., et al., (2006). Human SHPRH is a ubiquitin ligase for Mms2-Ubc13-dependent polyubiquitylation of proliferating cell nuclear antigen. *Proc. Natl. Acad. Sci. USA* **103**, 18107–18112. https://doi.org/10.1073/pnas.0608595103.
28. Unk, I., Hajdú, I., Fátyol, K., Hurwitz, J., Yoon, J.-H., Prakash, L., Prakash, S., Haracska, L., (2008). Human HLTF functions as a ubiquitin ligase for proliferating cell nuclear antigen polyubiquitination. *Proc. Natl. Acad. Sci. USA* **105**, 3768–3773. https://doi.org/10.1073/pnas.0800563105.
29. Blastyák, A., Hajdú, I., Unk, I., Haracska, L., (2010). Role of double-stranded DNA translocase activity of human HLTF in replication of damaged DNA. *Mol. Cell. Biol.* **30**, 684–693. https://doi.org/10.1128/MCB.00863-09.
30. Achar, Y.J., Balogh, D., Haracska, L., (2011). Coordinated protein and DNA remodeling by human HLTF on stalled replication fork. *Proc. Natl. Acad. Sci. USA* **108**, 14073–14078. https://doi.org/10.1073/pnas.1101951108.

31. Brühl, J., Trautwein, J., Schäfer, A., Linne, U., Bouazoune, K., (2019). The DNA repair protein SHPRH is a nucleosome-stimulated ATPase and a nucleosome-E3 ubiquitin ligase. *Epigenetics Chromatin.* **12** https://doi.org/10.1186/s13072-019-0294-5.
32. Motegi, A., Sood, R., Moinova, H., Markowitz, S.D., Liu, P. P., Myung, K., (2006). Human SHPRH suppresses genomic instability through proliferating cell nuclear antigen polyubiquitination. *J. Cell Biol.* **175**, 703–708. https://doi.org/10.1083/jcb.200606145.
33. Walker, J.E., Saraste, M., Runswick, M.J., Gay, N.J., (1982). Distantly related sequences in the alpha- and beta-subunits of ATP synthase, myosin, kinases and other ATP-requiring enzymes and a common nucleotide binding fold. *EMBO J.* **1**, 945–951. https://doi.org/10.1002/j.1460-2075.1982.tb01276.x.
34. Gangavarapu, V., Haracska, L., Unk, I., Johnson, R.E., Prakash, S., Prakash, L., (2006). Mms2-Ubc13-dependent and -independent roles of Rad5 ubiquitin ligase in postreplication repair and translesion DNA synthesis in Saccharomyces cerevisiae. *Mol. Cell. Biol.* **26**, 7783–7790. https://doi.org/10.1128/MCB.01260-06.
35. Ulrich, H.D., (2003). Protein-protein interactions within an E2-RING finger complex. Implications for ubiquitin-dependent DNA damage repair. *J. Biol. Chem.* **278**, 7051–7058. https://doi.org/10.1074/jbc.M212195200.
36. Parker, J.L., Ulrich, H.D., (2009). Mechanistic analysis of PCNA poly-ubiquitylation by the ubiquitin protein ligases Rad18 and Rad5. *EMBO J.* **28**, 3657–3666. https://doi.org/10.1038/emboj.2009.303.
37. Shen, M., Dhingra, N., Wang, Q., Cheng, C., Zhu, S., Tian, X., Yu, J., Gong, X., et al., (2021). Structural basis for the multi-activity factor Rad5 in replication stress tolerance. *Nature Commun.* **12**, 321. https://doi.org/10.1038/s41467-020-20538-w.
38. Liefshitz, B., Steinlauf, R., Friedl, A., Eckardt-Schupp, F., Kupiec, M., (1998). Genetic interactions between mutants of the "error-prone" repair group of Saccharomyces cerevisiae and their effect on recombination and mutagenesis (accessed May 21, 2019) *Mutat. Res.* **407**, 135–145 http://www.ncbi.nlm.nih.gov/pubmed/9637242.
39. Čejka, P., Vondrejs, V., Storchová, Z., (2001). Dissection of the functions of the Saccharomyces cerevisiae RAD6 postreplicative repair group in mutagenesis and UV sensitivity. *Genetics* **159**, 953–963. https://doi.org/10.1093/genetics/159.3.953.
40. Kuang, L., Kou, H., Xie, Z., Zhou, Y., Feng, X., Wang, L., Wang, Z., (2013). A non-catalytic function of Rev1 in translesion DNA synthesis and mutagenesis is mediated by its stable interaction with Rad5. *DNA Repair (Amst)* **12**, 27–37. https://doi.org/10.1016/j.dnarep.2012.10.003.
41. Xu, X., Lin, A., Zhou, C., Blackwell, S.R., Zhang, Y., Wang, Z., Feng, Q., Guan, R., et al., (2016). Involvement of budding yeast Rad5 in translesion DNA synthesis through physical interaction with Rev1. *Nucleic Acids Res.* **44**, 5231–5245. https://doi.org/10.1093/nar/gkw183.
42. Iyer, L.M., Babu, M.M., Aravind, L., (2006). The HIRAN domain and recruitment of chromatin remodeling and repair activities to damaged DNA. *Cell Cycle* **5**, 775–782. https://doi.org/10.4161/cc.5.7.2629.
43. Masuda, Y., Mitsuyuki, S., Kanao, R., Hishiki, A., Hashimoto, H., Masutani, C., (2018). Regulation of HLTF-mediated PCNA polyubiquitination by RFC and PCNA monoubiquitination levels determines choice of damage tolerance pathway. *Nucleic Acids Res.* **46**, 11340–11356. https://doi.org/10.1093/nar/gky943.
44. Achar, Y.J., Balogh, D., Neculai, D., Juhasz, S., Morocz, M., Gali, H., Dhe-Paganon, S., Venclovas, Č., et al., (2015). Human HLTF mediates postreplication repair by its HIRAN domain-dependent replication fork remodelling. *Nucleic Acids Res.* **43**, 10277–10291. https://doi.org/10.1093/nar/gkv896.
45. Kile, A.C., Chavez, D.A., Bacal, J., Eldirany, S., Korzhnev, D.M., Bezsonova, I., Eichman, B.F., Cimprich, K.A., (2015). HLTF's Ancient HIRAN Domain Binds 3' DNA Ends to Drive Replication Fork Reversal. *Mol. Cell.* **58**, 1090–1100. https://doi.org/10.1016/j.molcel.2015.05.013.
46. Chavez, D.A., Greer, B.H., Eichman, B.F., (2018). The HIRAN domain of helicase-like transcription factor positions the DNA translocase motor to drive efficient DNA fork regression. *J. Biol. Chem.* **293**, 8484–8494. https://doi.org/10.1074/jbc.RA118.002905.
47. Shin, S., Hyun, K., Kim, J., Hohng, S., (2018). ATP binding to Rad5 initiates replication fork reversal by inducing the unwinding of the leading arm and the formation of the Holliday Junction. *Cell Rep.* **23**, 1831–1839. https://doi.org/10.1016/j.celrep.2018.04.029.
48. Brash, D.E., Rudolph, J.A., Simon, J.A., Lin, A., Mckenna, G.J., Baden, H.P., Halperin, A.J., Pontén, J., (1991). A role for sunlight in skin cancer: UV-induced p53 mutations in squamous cell carcinoma. *Proc. Natl. Acad. Sci. USA* **88**, 10124–10128. https://doi.org/10.1073/pnas.88.22.10124.
49. Tessman, I., Liu, S.K., Kennedy, M.A., (1992). Mechanism of SOS mutagenesis of UV-irradiated DNA: Mostly error-free processing of deaminated cytosine. *Proc. Natl. Acad. Sci. USA* **89**, 1159–1163. https://doi.org/10.1073/pnas.89.4.1159.
50. Stary, A., Kannouche, P., Lehmann, A.R., Sarasin, A., (2003). Role of DNA polymerase η in the UV mutation spectrum in human cells. *J. Biol. Chem.* **278**, 18767–18775. https://doi.org/10.1074/jbc.M211838200.
51. Choi, J.H., Pfeifer, G.P., (2005). The role of DNA polymerase η in UV mutational spectra. *DNA Repair (Amst)* **4**, 211–220. https://doi.org/10.1016/j.dnarep.2004.09.006.
52. Yu, S.-L., Johnson, R.E., Prakash, S., Prakash, L., (2001). Requirement of DNA polymerase η for error-free bypass of UV-induced CC and TC photoproducts. *Mol. Cell. Biol.* **21**, 185–188. https://doi.org/10.1128/mcb.21.1.185-188.2001.
53. Pagès, V., Bresson, A., Acharya, N., Prakash, S., Fuchs, R.P., Prakash, L., (2008). Requirement of Rad5 for DNA polymerase ζ-dependent translesion synthesis in Saccharomyces cerevisiae. *Genetics* **180**, 73–82. https://doi.org/10.1534/genetics.108.091066.
54. Finley, D., Özkaynak, E., Varshavsky, A., (1987). The yeast polyubiquitin gene is essential for resistance to high temperatures, starvation, and other stresses. *Cell.* **48**, 1035–1046. https://doi.org/10.1016/0092-8674(87)90711-2.
55. Knop, M., Siegers, K., Pereira, G., Zachariae, W., Winsor, B., Nasmyth, K., Schiebel, E., (1999). Epitope tagging of yeast genes using a PCR-based strategy: more tags and improved practical routines. *Yeast* **15**, 963–972. https://doi.org/10.1002/(SICI)1097-0061(199907)15:10B<963::AID-YEA399>3.0.CO;2-W.

56. Frittmann, O., Gali, V.K., Halmai, M., Toth, R., Gyorfy, Z., Balint, E., Unk, I., (2021). The Zn-finger of Saccharomyces cerevisiae Rad18 and its adjacent region mediate interaction with Rad 5. *G3 Genes|Genomes|Genetics* **11** https://doi.org/10.1093/g3journal/jkab041.
57. Lea, D.E., Coulson, C.A., (1949). The distribution of the numbers of mutants in bacterial populations. *J. Genet.* **49**, 264–285. https://doi.org/10.1007/BF02986080.
58. Li, H., Durbin, R., (2010). Fast and accurate long-read alignment with Burrows-Wheeler transform. *Bioinformatics* **26**, 589–595. https://doi.org/10.1093/bioinformatics/btp698.
59. Li, H., Handsaker, B., Wysoker, A., Fennell, T., Ruan, J., Homer, N., Marth, G., Abecasis, G., Durbin, R., (2009). 1000 Genome Project Data Processing Subgroup, The Sequence Alignment/Map format and SAMtools. *Bioinformatics* **25**, 2078–2079. https://doi.org/10.1093/bioinformatics/btp352.
60. McKenna, A., Hanna, M., Banks, E., Sivachenko, A., Cibulskis, K., Kernytsky, A., Garimella, K., Altshuler, D., et al., (2010). The Genome Analysis Toolkit: a MapReduce framework for analyzing next-generation DNA sequencing data. *Genome Res.* **20**, 1297–1303. https://doi.org/10.1101/gr.107524.110.
61. Garrison, E., Kronenberg, Z.N., Dawson, E.T., Pedersen, B.S., Prins, P., (2021). Vcflib and tools for processing the VCF variant call format. *BioRxiv*. 10.1101/2021.05.21.445151.
62. Ulrich, H.D., Davies, A.A., (2009). In Vivo Detection and Characterization of Sumoylation Targets in Saccharomyces cerevisiae. *Methods Mol. Biol.*, 81–103. https://doi.org/10.1007/978-1-59745-566-4_6.